



Published in final edited form as:

Biochim Biophys Acta. 2009 February ; 1788(2): 450–457. doi:10.1016/j.bbamem.2008.09.014.

Cytoskeleton reorganization in influenza hemagglutinin–initiated syncytium formation

Jean-Philippe Richard^{*}, Eugenia Leikina^{*}, and Leonid V. Chernomordik^{*}

^{*} *Section on Membrane Biology, Laboratory of Cellular and Molecular Biophysics, Eunice Kennedy Shriver National Institute of Child Health and Human Development, National Institutes of Health, Bethesda, MD 20892-1855, USA*

Abstract

Little is known about the mechanisms of cell-cell fusion in development and diseases and, especially, about fusion stages downstream an opening of nascent fusion pore(s). Earlier works on different cell-cell fusion reactions have indicated that cytoskeleton plays important role in syncytium formation. However, due to complexity of these reactions and multifaceted contributions of cytoskeleton in cell physiology, it has remained unclear whether cytoskeleton directly drives fusion pore expansion or affects preceding fusion stages. Here we explore cellular reorganization associated with fusion pore expansion in syncytium formation using relatively simple experimental system. Fusion between murine embryonic fibroblasts NIH3T3-based cells is initiated on demand by well-characterized fusogen influenza virus hemagglutinin. We uncouple early fusion stages dependent on protein fusogens from subsequent fusion pore expansion stage and establish that the transition from local fusion to syncytium requires metabolic activity of living cells. Effective syncytium formation for cells with disorganized actin and microtubule cytoskeleton argues against hypothesis that cytoskeleton drives fusion expansion.

Keywords

cytoskeleton; membrane fusion; syncytium; influenza hemagglutinin

INTRODUCTION

Membrane fusion is a critical event in biology. Exocytosis, protein trafficking, and entry of enveloped viruses involve membrane fusion [1,2]. Moreover, fusion between cells plays key roles in development as in sperm–oocyte fusion, trophoblast cell fusion, and the formation of myotubes, osteoclasts, and giant cells [3,4]. Finally, fusion between somatic cells and embryonic stem cells is an intriguing phenomenon in physiology and an important tool in stem cell research [5].

Intracellular and intercellular fusion reactions have been extensively studied in many experimental systems. The focus of this research has been on identification of the proteins involved and on the mechanisms by which these proteins connect the membrane-enclosed

Correspondence to: Dr. Leonid V. Chernomordik, Building 10, Room 10D04, 10 Center Drive, Bethesda, MD 20892-1855; Tel: 301-594-1128; Fax: 301-480-2916; e-mail: chernoml@mail.nih.gov.

Publisher's Disclaimer: This is a PDF file of an unedited manuscript that has been accepted for publication. As a service to our customers we are providing this early version of the manuscript. The manuscript will undergo copyediting, typesetting, and review of the resulting proof before it is published in its final citable form. Please note that during the production process errors may be discovered which could affect the content, and all legal disclaimers that apply to the journal pertain.

volumes with nascent nanometer-sized fusion pores. By contrast, the extension of these pores and the cellular reorganization that in the case of cell-cell fusion yield a syncytium have remained poorly understood. Since cell shape and its changes are mainly determined by the cytoskeleton, several studies have focused on its role during syncytium formation, implicating either the actin or the microtubule network [6–15]. However, even for the same experimental system, fusion between *Drosophila* myoblasts, the specific role of the actin cytoskeleton: providing the driving force for fusion pore extension [16], priming cells for fusion initiation [17], or restricting membrane rearrangements [18], remains to be clarified.

Due to the complexity of developmental cell fusion reactions and a large number of proteins involved in controlling both pre- and post- fusion stages, it is very hard to distinguish contributions of cytoskeleton rearrangements during fusion pore expansion from those at the preceding stages of cell-cell binding, plasma membrane expression of yet unknown fusogens, their activation, and, finally, fusion pore opening. In this work we address the fundamental question whether cytoskeleton drives syncytium formation, using an experimental system that is much simpler than cell fusion in development. A robust and relatively fast fusion reaction between mammalian cells is initiated here by a low pH-triggered restructuring of one of the best-characterized protein fusogens influenza virus hemagglutinin (HA).

The opening of initial fusion pores by low-pH forms of HA mimics fusion between the viral envelope and the membrane of an acidified endosome during virus entry. HA structure, its changes at the pH of fusion, and the HA-mediated pathway that culminates in a fusion pore opening have been studied in considerable detail [19–22,23,24]. Here, we utilize HA to initiate fusion, but we concentrate on the transition from early fusion pores to expanding cytoplasmic cell-cell connections readily detectable with fluorescence microscopy. While the opening of fusion pores requires only the presence of functional HA, this transition requires cell metabolic energy and is negatively regulated by protein kinase C (PKC). Late and cell-dependent stages of fusion yielding syncytium formation are not blocked by microtubule- and actin-modifying treatments, indicating that neither the microtubule nor the actin cytoskeleton drives the enlargement of initial fusion connections.

MATERIALS AND METHODS

Reagents

Jasplakinolide and latrunculin A were purchased from Invitrogen. Nocodazole, colchicine, taxol (paclitaxel), sodium azide (NaN_3), 2-deoxy-D-glucose, cytochalasin D, 2, 3-butanedione monoxime (BMD), and blebbistatin were purchased from Sigma-Aldrich. Phorbol 12-myristate 13-acetate (PMA), bisindolylmaleimide I, and staurosporine were purchased from Calbiochem.

Cell culture and preparation

NIH 3T3 cells (murine embryonic fibroblasts) and HAb2 cells (NIH 3T3 cells stably expressing HA [25]) were cultured as exponentially growing subconfluent monolayers on 90-mm plates in DMEM supplemented with Glutamax (Invitrogen) and 10% (v/v) fetal bovine serum. Exponentially growing cells were dissociated with trypsin (Invitrogen). The cells (2.5×10^5) were plated and cultured overnight on 30-mm plates in the presence of 2.5 mM sodium butyrate to potentiate expression of HA [26,27]. In some experiments, we used human erythrocyte ghosts labeled with fluorescent lipid PKH26 (Sigma, St. Louis, MO) and an aqueous dye, 6-carboxyfluorescein (Invitrogen, Carlsbad, CA), prepared for experiments as described in [22].

Fusion assay

To prepare them for fusion, HAb2 cells were pretreated with trypsin (5 $\mu\text{g}/\text{ml}$, 5 min, 37°C) to cleave the fusion-inactive precursor of HA (HA0) to its fusion active (HA1-S-S-HA2) form [28]. The cells were washed twice with PBS with Ca/Mg and exposed for 5 min to pH 4.9 medium at 37°C, in order to trigger fusogenic conformational change in HA. Cells were washed two more times with PBS and incubated for 2 h in DMEM supplemented with serum. In the experiments in which we combined low temperature incubation with latrunculin treatment (Figure 7B), trypsin pretreatment was followed by additional 1-h incubation in PBS with Ca/Mg at 37°C, and then proceed to fusion experiments.

Fluorescence microscopy

The different experiments were performed as described in the figure legends. In the experiments with fixed cells, Invitrogen's protocol was used concerning the use of Alexa488-Phalloidin (Invitrogen). Tubulin was labeled using mouse anti-alpha tubulin antibody, with alexa594 donkey anti-mouse antibody as secondary antibody (both Invitrogen). The distribution of fluorescence was analyzed on an Olympus IX70 inverted fluorescence microscope.

Syncytium assay

Two hours after the end of the low-pH application, cells were labeled with Hoechst (Invitrogen) and orange cell tracker (Invitrogen) in order to better visualize their contour. Then, we analyzed five random fields for each sample. The syncytium index for each sample was determined as the number of nuclei in a multinucleated cell divided by the total number of nuclei in the field. To verify that the formation of multinucleated cells involved cell fusion, in some experiments (Figure 1) we labeled half of the cells with green cell tracker and half with orange (both cell trackers were purchased from Invitrogen), mixed them, and grew the cells together overnight before the trypsin/low-pH treatment. We scored cells as syncytia if they had multiple nuclei in a single cell volume or if the connections between fusing cells appeared to be large enough to allow nucleus passage. Each graph is representative of data from one of three independent experiments. For graphs that represent normalized data, at least three independent experiments were performed.

RESULTS

Experimental system

A number of earlier studies characterized HA-mediated fusion between HAb2 cells and erythrocytes [26,29]. In this work to explore the formation of multinucleate cells, we have focused on fusion between HAb2 cells. These cells have the typical cytoskeleton of attached cells, with cortical actin, actin stress fibers, and microtubules (see below). Neighboring HAb2 cells contact each other through a narrow motile lamellipodium sent from one cell to the body of another cell. Pre-fusion contacts through lamellipodia are an important feature of some biologically relevant fusion reactions, such as the formation of multinucleate macrophages [30].

We always find some background of binucleated cells, and rarely also tri-nucleated cells, which likely represent dividing cells. As expected, the numbers of these multinucleated cells does not change in the control experiments with HAb2 cells not treated with low pH, or treated with low pH without the trypsin pre-treatment that is required for transforming HA into a fusion-competent form (not shown). In contrast, a short-term treatment of a low-pH medium to trypsin-treated HAb2 cells yields many multinucleated cells. These cells are formed by fusion, since they contain both of the cell trackers that initially are separated between different cell

populations (Figure 1). Opening of fusion pores detected as redistribution of the probes and thus appearance of double labeled cells is observed already at 5 min after low pH application. However, the gradual enlargement of intercellular connections and changes in cell shapes towards syncytium formation develops much slower.

While we find that HAb2 cells are capable of forming syncytia by fusing with parental NIH 3T3 cells that do not express HA (data not shown), all data presented below are obtained for fusion between HAb2 cells. For these cells, 60 min after the end of low-pH application, between 25% and 100% of all nuclei are in syncytia. The day-to-day variability in the percentage of cells in syncytia after a low pH pulse and in the number of multinucleated cells in our negative control experiments (no low pH application) likely reflect the differences in the state of cell cultures and the levels of HA expression. Therefore, each of the presented sets of experiments includes its own negative and positive controls.

Rapid and synchronized committing of many cells to fusion allows us to focus on the unexplored late stages of syncytium formation.

Syncytium formation requires metabolic activity of living cells

Slowing down metabolism, either by lowering the cell-incubation temperature to 4°C or by depleting ATP pools by pre-treating cells with NaN₃ and 2-deoxy-D-glucose is often used to determine the energy-dependency of a cellular process.

No syncytia are observed for cells chilled to 4°C immediately after a low-pH pulse. Even after 2 h of incubation at 4°C, the bound cells remain distinct rather than multinucleated (Figure 2A). Raising the temperature to 37°C yields the same percentage of cells in syncytia as that observed when the cells are incubated at 37°C during the entire experiment, suggesting that low temperature blocks only late fusion stages. Similarly, in the experiments carried out entirely at 37°C, depletion of intracellular ATP pools of HAb2 cells by a combination of NaN₃ and 2-D-deoxyglucose completely inhibits syncytium formation (Figure 2B).

Neither ATP depletion nor incubation at 4°C inhibits early fusion stages. Prior to a low-pH application, we incubate the ATP-depleted cells or the cells incubated at the cold temperature with a small number of erythrocyte ghosts labeled with membrane and content probes. After the low-pH application, we observe spreading of the dyes from an erythrocyte (RBC) to the HAb2 cell that this RBC is bound to. The dye spreads then to neighboring HAb2 cells that do not have bound fluorescent RBCs (Supplemental Figure S1). This strategy allows us during experiments to deliver dyes to one of the fusing HAb2 cells and then to monitor spreading of dyes between fusing HAb2 cells. Cell-to-cell transfer of fluorescent probes in the absence of a syncytium indicates that ATP depletion blocks cell fusion downstream of the opening of the initial fusion pores.

The conclusion that syncytium formation is not spontaneous but rather involves cell machinery is further substantiated by experiments with reagents modifying activity of protein kinase C (PKC), a key regulator of cell physiology (Figure 2C). PMA, a promoter of PKC, and bisindolylmaleimide I and staurosporine, PKC inhibitors [31], respectively inhibits and promote cell-cell fusion, suggesting that syncytium formation is negatively regulated by PKC. We cannot at present identify the mechanism involved, since PKC directly or indirectly regulates quite a few of the important biochemical pathways [32].

To summarize, in contrast to early fusion stages, syncytium formation proceeds only in metabolically active cells. This finding is in agreement with earlier studies on syncytium formation induced by different viral fusogens or by electroporation [6,33,34].

Microtubules in syncytium formation

To explore rearrangements of the microtubular network during fusion between HAb2 cells, we fix the cells at different times after the end of the low-pH application and visualize alpha tubulin structures with fluorescent antibodies (Figure 3). In untreated cells, we observe, as expected, distinct microtubule bundles originating from microtubules organizing center (MTOC) in the vicinity of nuclei. As soon as 5 min after low pH application, microtubules labeling in fusing cells becomes more diffused. Fusion between HAb2 cells results thus in a rearrangement of the whole structure and shape of the microtubule cytoskeleton. We observe no bundles of microtubules passing through the expanding fusion pores. Even 2 h after the low-pH application, when syncytium formation and the microtubule rearrangements appear to be completed, we observe multinucleated cells containing multiple microtubules organizing centers (MTOC) located away from the gathered nuclei.

To test whether the microtubular network plays a functional role in syncytium formation, HAb2 cells were pre-treated with the microtubule-stabilizing agent taxol or with the microtubule-destabilizing agent nocodazole (Figure 4). As expected, these drugs cause major disorganization of the microtubule network of the cells (Supplemental Figure S2A–C). However, syncytium formation is inhibited neither by taxol (Figure 4A) nor by nocodazole (Figure. 4B). Interestingly, nocodazole does not prevent the gathering of nuclei in syncytia (Supplemental Figure S2B). Colchicine, another microtubule-destabilizing agent, also does not inhibit syncytium formation (not shown).

Since disturbing the normal function and structure of the microtubular network does not block syncytium formation for HAb2 cells, we conclude that microtubules and microtubule-dependent vesicle transport do not play a major role in the expansion of fusion pores.

Actin-cytoskeleton rearrangements during syncytium formation

Many important properties of cell membranes are controlled by their interactions with the actin cytoskeleton and, especially, with the actin-based contractile cortex under the plasma membrane. The actin cytoskeleton might generate force through myosin-dependent contraction or actin polymerization [35], and it has been hypothesized that fusion pores are expanded by actin bundles assembled at the arc-shaped edges of the pores [36].

Preparation of HAb2 cells for fusion includes incubation with trypsin. We find trypsin application to cause a very fast disassembly of the actin cortex and internal stress fibers (Figure 5). This disassembly might involve activation of protease receptors on the cell surface described in [37]. Thus, at the time of fusion-triggering low-pH application, the actin cytoskeleton is very much disorganized. Fifteen minutes after the end of the low-pH pulse, the actin cytoskeleton structures visibly recover and reorganize to fit the shape of the newly formed entity. We never observe actin stress fibers invading the expanding lumen connecting two fusing cells. Two hours after the low-pH pulse application, strong cortical actin staining and stress fibers can be detected in all multinucleated cells.

In brief, we observe no accumulation of actin cytoskeleton inside or underneath the fusion pores, arguing against a role of actin bundles assembled at the edges of the fusion pores suggested in [36].

Effects of actin-modifying treatments

To further explore the possible involvement of the actin cytoskeleton in syncytium formation, we disturb actin structures in HAb2 cells with actin depolymerizing (cytochalasin D and latrunculin A) or actin polymerizing (jasplakinolide) reagents [38]. Note that jasplakinolide under our conditions is also expected to disorder the actin cytoskeleton [39]. The concentrations

of actin-modifying reagents in these experiments are within the ranges recommended by Invitrogen protocols and used in earlier studies ([40] and [39], [41], [42] and [7]). While neither of these reagents prevents HA-initiated syncytium formation (Figure 6), quantitative comparison of syncytium formation with or without these treatments is hindered by the agent-induced changes in cell shapes (cells become rounder) that disturb cell-cell contacts and thus affect early fusion stages.

In another experimental approach, we pre-incubate HAb2 cells at 4°C for 1 h prior to the application of low pH (Figure 7A). This pre-treatment leads to a profound disassembly of the actin cytoskeleton (as confirmed by labeling of fixed cells with fluorescent phalloidin, Supplemental figure S3), with no apparent change in cell-cell contacts. Disorganization of actin structures at the time of low-pH application does not inhibit syncytium formation. At the opposite, we observe a small but reproducible promotion.

In the experimental design described above, fusion is initiated by treating cells with warm (37°C) acidic medium; and, thus, syncytium formation develops at the time when the actin cytoskeleton starts to recover. To verify that syncytium formation develops even when such recovery is blocked, we follow low-temperature-induced dissociation of the actin cytoskeleton with application of latrunculin A, a strong actin depolymerizing agent (Figure 7B). HAb2 cells are treated with trypsin for 5 min and incubated for 1 h in PBS at 37°C with Ca/Mg in order to recover actin cytoskeleton- and lamellipodium-mediated contacts between the neighboring cells. Cells are then treated for 5 min with low pH at 37°C to allow all cell pairs destined to fuse to have nascent fusion pores already open [43]. The cells are then incubated at 4°C for 1 h in order to disassemble the actin cytoskeleton, and, finally, the temperature is raised to 37°C in the presence or absence of latrunculin A. The syncytium index is monitored 2 h after that.

In the control experiments, to evaluate the degree of recovery of the actin cytoskeleton after raising the temperature, we fix the cells at different times (0, 5, 15, 30, 60, and 120 min) and label them with Alexafluor488-tagged phalloidin. While 15 min at 37°C in the absence of latrunculin is sufficient to completely restore the actin cytoskeleton, we never observe actin structure recovery in the presence of latrunculin (data not shown).

Thus, in the experiments where actin cortex has been dissociated at the onset of fusion and remains dissociated throughout the fusion pore expansion, fusion yields efficient syncytium formation (Figure 7B). These findings, along with the results in Figure 7A, argue against the hypothesis that actin cytoskeleton drives the expansion. On the contrary, as shown in the experiments presented in Figure 7A, we observe a slight increase in the number of multinucleated cells suggesting that actin cytoskeleton, if anything, restricts syncytium formation.

Generation of force by the actin cortex beneath the plasma membranes might involve myosin-dependent contraction [44]. In addition, properties of the actin cortex under the plasma membrane might be modulated by myosin II-driven contraction [45]. To explore whether syncytium formation depends on myosin activity, we use two inhibitors of non-muscle myosin II: blebbistatin and BMD (Figure 7C) [46–48]. Neither of these reagents has an effect on the efficiency of syncytium formation.

To summarize, syncytium formation in cells with depolymerized actin structures and inhibited active contraction proceeds with at least the same efficiency as in control cells, arguing against hypothesis that actin cytoskeleton drives the expansion of fusion pores.

DISCUSSION

Cell-cell fusion plays an important role in development (for instance, sperm-egg fusion and myotube formation), throughout our lives (fusion of macrophages), and in pathophysiology (viral syncytia). The mechanisms by which fusion pores generated by specialized proteins expand to connect cells by a passage wide enough to allow redistribution of cell nuclei are poorly understood. Our experimental system of HA-initiated syncytium formation based on a well characterized and easy to trigger fusogen provides a controlled way of forming fusion pores and, thus, facilitates analysis of the mechanisms of their expansion. In contrast to many developmental cell-cell fusion models, our system is based on mammalian cells in order to minimize potential orthology problems [49,50]. Furthermore, while in an important mammalian syncytium model of myoblast fusion the multistep cascades of regulation only yield detectable syncytia at least 12 h after triggering [49,51], we can already specifically study cellular reorganization downstream of fusion pores opening to yield syncytia within 1 h after triggering.

We explore whether fusion pore extension yielding syncytia requires any contribution of the cells or whether the opening of a fusion pore detectable with light microscopy signifies an irreversible commitment to syncytium formation (with subsequent stages to proceed spontaneously). Finding that metabolic inhibitors such as low temperature or ATP depletion block transition from early fusion intermediates to formed syncytia suggests that syncytium formation is controlled by cell machinery. In the experiments in which fusion is blocked by lowering of the temperature to 4°C immediately after fusion pore opening, lifting the block 1 h later by raising the temperature to 37°C fully restores the syncytium index. This finding suggests that the small pore(s) in between the two fusing cells remain(s) open and are just waiting for the cells to continue the syncytium formation process by providing sufficient energy for the internal rearrangements to occur. The importance of the cell machinery in syncytium formation is further emphasized by studying the effects of reagents modifying PKC activity. PKC is central to many regulatory pathways in cells, including the regulation of actin reorganization [52,53] and of cell machinery involved in membrane trafficking [54]. Specific mechanisms of negative regulation of syncytium formation by PKC and PKC isoforms involved remain to be clarified. However, the fact of cell fusion dependence on PKC activity strengthens the conclusion that after protein fusogens have carried out their job of opening fusion pores, the subsequent fusion stages are controlled by cell physiology.

Early studies on electrofusion [6] and a more recent work on myoblast formation [55] suggested that microtubule dynamics and microtubule-associated proteins play an important role in syncytium formation. The microtubule cytoskeleton is important in organizing intracellular compartments. Microtubules interact with the Golgi apparatus, the endoplasmic reticulum, and also endo- and exocytotic vesicles. It has been proposed that microtubules invade the cytoplasmic bridge between the fusing cells, connect the two nuclei and drive pore expansion and the subsequent cellular reorganization [6]. However, our data with drugs over-stabilizing or destroying microtubules argue against this hypothesis and indicate that the microtubule cytoskeleton is not necessary for syncytium formation to proceed. Moreover, we never observe a significant strengthening of microtubular network in syncytium formation during time-lapse experiments with fixed cells. Interestingly, the microtubule cytoskeleton, after 2 h of incubation in DMEM supplemented with serum at 37°C, seems fully restored despite MTOC misplacement.

In our system, microtubule-modifying drugs have no effect on the circular nucleus gathering after cell fusion, as presented in Supplemental Figure S4. The mechanisms that underlie this gathering are yet unclear. Nucleus movement in cells has been proposed to be driven by either microtubule or actin- cytoskeleton [15, 56, 57], and our findings indicate that functional

microtubular network is not a prerequisite for the nuclei gathering. In addition, we never observe fusion between nuclei in any experiment, each of them keeping its own individuality after fusion.

Cell shape is highly dependent on the actin cytoskeleton, as the plasma membrane lies on a cortical actin meshwork [58]. The actin cytoskeleton supports transformations in cell shape such as membrane bending into lamellipodia, filopodia, or simply microspikes. Here, we explore the role of the actin cytoskeleton in syncytium formation. Our finding that actin-modifying reagents and treatments as well as myosin inhibitors do not inhibit HA-initiated syncytium formation argue against the hypothesis that enlargement of the cytoplasmic connection between fusing cells is driven by actin structure [16]. Moreover, a slight increase in syncytium formation for the cells with depolymerized actin cytoskeletons (Figure 7A and B) suggests that actin structures restrain cellular reorganization into syncytia. Interestingly, dissociation of the cytoskeleton has been reported to facilitate several membrane remodeling processes. Disruption of membrane skeleton of erythrocytes is found to promote HA-mediated fusion between viral particles and erythrocytes [59]. Experiments with locally applied actin-modifying agents demonstrate that actin depolymerization along the cleavage furrow is important for furrow ingression during cytokinesis [60]. Local disassembly of the actin cortex also plays an important role in exocytosis, allowing intracellular vesicles to fuse with the plasma membrane [61].

In conclusion, we have proved that transition from early HA-initiated fusion stages to syncytium formation is an active process requiring energy provided by the cell machinery and is dependent on PKC regulation signaling cascades. Efficient syncytium formation observed for the cells treated with reagents that modify microtubule and actin structures argues against the hypothesis that the late stages of cell-cell fusion are driven by cytoskeleton. The dependence of late fusion stages on metabolic activity of living cells and syncytium formation for cells with depolymerized actin skeleton have been also observed for fusion initiated by baculovirus gp64, another protein fusogen [62].

The mechanistic insights provided by our simplified experimental model based on well characterized viral fusogens will hopefully help in elucidation of complex cell-cell fusion reactions in development and pathophysiology.

Supplementary Material

Refer to Web version on PubMed Central for supplementary material.

Acknowledgements

We thank A. Bershadsky, A. Chen, L. Joubert-Mang, M. Kozlov, B. Lebleu, K. Melikov, B. Podbilewicz, E. Zaitseva, and J. Zimmerberg for very helpful discussions. This research was supported by the Intramural Research Program of the NIH, NICHD.

References

1. Jahn R, Lang T, Sudhof TC. Membrane fusion. *Cell* 2003;112:519–533. [PubMed: 12600315]
2. Earp LJ, Delos SE, Park HE, White JM. The many mechanisms of viral membrane fusion proteins. *Current topics in microbiology and immunology* 2005;285:25–66. [PubMed: 15609500]
3. Chen EH, Grote E, Mohler W, Vignery A. Cell-cell fusion. *FEBS letters* 2007;581:2181–2193. [PubMed: 17395182]
4. Vignery A. Osteoclasts and giant cells: macrophage-macrophage fusion mechanism. *International journal of experimental pathology* 2000;81:291–304. [PubMed: 11168677]

5. Cowan CA, Atienza J, Melton DA, Eggan K. Nuclear reprogramming of somatic cells after fusion with human embryonic stem cells. *Science (New York, NY)* 2005;309:1369–1373.
6. Zheng QA, Chang DC. Reorganization of cytoplasmic structures during cell fusion. *Journal of cell science* 1991;100(Pt 3):431–442. [PubMed: 1808197]
7. Pontow SE, Heyden NV, Wei S, Ratner L. Actin cytoskeletal reorganizations and coreceptor-mediated activation of rac during human immunodeficiency virus-induced cell fusion. *J Virol* 2004;78:7138–7147. [PubMed: 15194790]
8. Schowalter RM, Wurth MA, Aguilar HC, Lee B, Moncman CL, McCann RO, Dutch RE. Rho GTPase activity modulates paramyxovirus fusion protein-mediated cell-cell fusion. *Virology* 2006;350:323–334. [PubMed: 16500690]
9. DeFife KM, Jenney CR, Colton E, Anderson JM. Disruption of filamentous actin inhibits human macrophage fusion. *Faseb J* 1999;13:823–832. [PubMed: 10224226]
10. Sylwester A, Wessels D, Anderson SA, Warren RQ, Shutt DC, Kennedy RC, Soll DR. HIV-induced syncytia of a T cell line form single giant pseudopods and are motile. *J Cell Sci* 1993;106(Pt 3):941–953. [PubMed: 8308076]
11. Kallewaard NL, Bowen AL, Crowe JE Jr. Cooperativity of actin and microtubule elements during replication of respiratory syncytial virus. *Virology* 2005;331:73–81. [PubMed: 15582654]
12. Gallo SA, Finnegan CM, Viard M, Raviv Y, Dimitrov A, Rawat SS, Puri A, Durell S, Blumenthal R. The HIV Env-mediated fusion reaction. *Biochim Biophys Acta* 2003;1614:36–50. [PubMed: 12873764]
13. Straube A, Merdes A. EB3 regulates microtubule dynamics at the cell cortex and is required for myoblast elongation and fusion. *Curr Biol* 2007;17:1318–1325. [PubMed: 17658256]
14. Wang E, Connolly JA, Kalnins VI, Choppin PW. Relationship between movement and aggregation of centrioles in syncytia and formation of microtubule bundles. *Proc Natl Acad Sci U S A* 1979;76:5719–5723. [PubMed: 293675]
15. Wang E, Cross RK, Choppin PW. Involvement of microtubules and 10-nm filaments in the movement and positioning of nuclei in syncytia. *The Journal of cell biology* 1979;83:320–337. [PubMed: 227913]
16. Massarwa R, Carmon S, Shilo BZ, Schejter ED. WIP/WASp-based actin-polymerization machinery is essential for myoblast fusion in *Drosophila*. *Dev Cell* 2007;12:557–569. [PubMed: 17419994]
17. Kim S, Shilagardi K, Zhang S, Hong SN, Sens KL, Bo J, Gonzalez GA, Chen EH. A critical function for the actin cytoskeleton in targeted exocytosis of prefusion vesicles during myoblast fusion. *Dev Cell* 2007;12:571–586. [PubMed: 17419995]
18. Richardson BE, Beckett K, Nowak SJ, Baylies MK. SCAR/WAVE and Arp2/3 are crucial for cytoskeletal remodeling at the site of myoblast fusion. *Development (Cambridge, England)* 2007;134:4357–4367.
19. White J, Kartenbeck J, Helenius A. Membrane fusion activity of influenza virus. *The EMBO journal* 1982;1:217–222. [PubMed: 7188182]
20. Nir S, Duzgunes N, de Lima MC, Hoekstra D. Fusion of enveloped viruses with cells and liposomes. Activity and inactivation. *Cell biophysics* 1990;17:181–201. [PubMed: 1705483]
21. Markosyan RM, Melikyan GB, Cohen FS. Tension of membranes expressing the hemagglutinin of influenza virus inhibits fusion. *Biophys J* 1999;77:943–952. [PubMed: 10423439]
22. Chernomordik LV, Frolov VA, Leikina E, Bronk P, Zimmerberg J. The pathway of membrane fusion catalyzed by influenza hemagglutinin: restriction of lipids, hemifusion, and lipidic fusion pore formation. *The Journal of cell biology* 1998;140:1369–1382. [PubMed: 9508770]
23. Zimmerberg J, Blumenthal R, Sarkar DP, Curran M, Morris SJ. Restricted movement of lipid and aqueous dyes through pores formed by influenza hemagglutinin during cell fusion. *The Journal of cell biology* 1994;127:1885–1894. [PubMed: 7806567]
24. Skehel JJ, Wiley DC. Receptor binding and membrane fusion in virus entry: the influenza hemagglutinin. *Annual review of biochemistry* 2000;69:531–569.
25. Doxsey SJ, Sambrook J, Helenius A, White J. An efficient method for introducing macromolecules into living cells. *The Journal of cell biology* 1985;101:19–27. [PubMed: 2989298]

26. Danieli T, Pelletier SL, Henis YI, White JM. Membrane fusion mediated by the influenza virus hemagglutinin requires the concerted action of at least three hemagglutinin trimers. *The Journal of cell biology* 1996;133:559–569. [PubMed: 8636231]
27. Markovic I, Leikina E, Zhukovsky M, Zimmerberg J, Chernomordik LV. Synchronized activation and refolding of influenza hemagglutinin in multimeric fusion machines. *The Journal of cell biology* 2001;155:833–844. [PubMed: 11724823]
28. Wiley DC, Skehel JJ. The structure and function of the hemagglutinin membrane glycoprotein of influenza virus. *Annual review of biochemistry* 1987;56:365–394.
29. Chernomordik LV, Leikina E, Frolov V, Bronk P, Zimmerberg J. An early stage of membrane fusion mediated by the low pH conformation of influenza hemagglutinin depends upon membrane lipids. *The Journal of cell biology* 1997;136:81–93. [PubMed: 9008705]
30. Jay SM, Skokos E, Laiwalla F, Krady MM, Kyriakides TR. Foreign body giant cell formation is preceded by lamellipodia formation and can be attenuated by inhibition of Rac1 activation. *Am J Pathol* 2007;171:632–640. [PubMed: 17556592]
31. Way KJ, Chou E, King GL. Identification of PKC-isoform-specific biological actions using pharmacological approaches. *Trends in pharmacological sciences* 2000;21:181–187. [PubMed: 10785652]
32. Breitkreutz D, Braiman-Wiksmann L, Daum N, Denning MF, Tennenbaum T. Protein kinase C family: on the crossroads of cell signaling in skin and tumor epithelium. *Journal of cancer research and clinical oncology* 2007;133:793–808. [PubMed: 17661083]
33. Kempf C, Kohler U, Michel MR, Koblet H. Semliki Forest virus-induced polykaryocyte formation is an ATP-dependent event. *Archives of virology* 1987;95:111–122. [PubMed: 3592981]
34. Okada Y. Sendai virus-induced cell fusion. *Methods in enzymology* 1993;221:18–41. [PubMed: 8395633]
35. Even-Ram S, Doyle AD, Conti MA, Matsumoto K, Adelstein RS, Yamada KM. Myosin IIA regulates cell motility and actomyosin-microtubule crosstalk. *Nature cell biology* 2007;9:299–309.
36. Zheng QA, Chang DC. Dynamic changes of microtubule and actin structures in CV-1 cells during electrofusion. *Cell motility and the cytoskeleton* 1990;17:345–355. [PubMed: 2076549]
37. Pollack R, Rifkin D. Actin-containing cables within anchorage-dependent rat embryo cells are dissociated by plasmin and trypsin. *Cell* 1975;6:495–506.
38. Eitzen G. Actin remodeling to facilitate membrane fusion. *Biochimica et biophysica acta* 2003;1641:175–181. [PubMed: 12914958]
39. Bubb MR, Spector I, Beyer BB, Fosen KM. Effects of jasplakinolide on the kinetics of actin polymerization. An explanation for certain *in vivo* observations. *The Journal of biological chemistry* 2000;275:5163–5170. [PubMed: 10671562]
40. Coue M, Brenner SL, Spector I, Korn ED. Inhibition of actin polymerization by latrunculin A. *FEBS letters* 1987;213:316–318. [PubMed: 3556584]
41. Morales M, Colicos MA, Goda Y. Actin-dependent regulation of neurotransmitter release at central synapses. *Neuron* 2000;27:539–550. [PubMed: 11055436]
42. Carbajal ME, Vitale ML. The cortical actin cytoskeleton of lactotropes as an intracellular target for the control of prolactin secretion. *Endocrinology* 1997;138:5374–5384. [PubMed: 9389523]
43. Mittal A, Leikina E, Bentz J, Chernomordik LV. Kinetics of influenza hemagglutinin-mediated membrane fusion as a function of technique. *Analytical biochemistry* 2002;303:145–152. [PubMed: 11950214]
44. Charras GT, Hu CK, Coughlin M, Mitchison TJ. Reassembly of contractile actin cortex in cell blebs. *The Journal of cell biology* 2006;175:477–490. [PubMed: 17088428]
45. Bresnick AR. Molecular mechanisms of nonmuscle myosin-II regulation. *Current opinion in cell biology* 1999;11:26–33. [PubMed: 10047526]
46. Kolega J, Taylor DL. Gradients in the concentration and assembly of myosin II in living fibroblasts during locomotion and fiber transport. *Molecular biology of the cell* 1993;4:819–836. [PubMed: 8241568]
47. Kovacs M, Toth J, Hetenyi C, Malnasi-Csizmadia A, Sellers JR. Mechanism of blebbistatin inhibition of myosin II. *The Journal of biological chemistry* 2004;279:35557–35563. [PubMed: 15205456]

48. Yarrow JC, Lechler T, Li R, Mitchison TJ. Rapid de-localization of actin leading edge components with BDM treatment. *BMC cell biology* 2003;4:5. [PubMed: 12783627]
49. Horsley V, Pavlath GK. Forming a multinucleated cell: molecules that regulate myoblast fusion. *Cells, tissues, organs* 2004;176:67–78. [PubMed: 14745236]
50. Towler MC, Kaufman SJ, Brodsky FM. Membrane traffic in skeletal muscle. *Traffic (Copenhagen, Denmark)* 2004;5:129–139.
51. Mohler WA, Blau HM. Gene expression and cell fusion analyzed by lacZ complementation in mammalian cells. *Proceedings of the National Academy of Sciences of the United States of America* 1996;93:12423–12427. [PubMed: 8901597]
52. Eitzen G, Wang L, Thorngren N, Wickner W. Remodeling of organelle-bound actin is required for yeast vacuole fusion. *The Journal of cell biology* 2002;158:669–679. [PubMed: 12177043]
53. Yu HY, Bement WM. Control of local actin assembly by membrane fusion-dependent compartment mixing. *Nature cell biology* 2007;9:149–159.
54. Alvi F, Idkowiak-Baldys J, Baldys A, Raymond JR, Hannun YA. Regulation of membrane trafficking and endocytosis by protein kinase C: emerging role of the pericentration, a novel protein kinase C-dependent subset of recycling endosomes. *Cell Mol Life Sci* 2007;64:263–270. [PubMed: 17180302]
55. McElhinny AS, Perry CN, Witt CC, Labeit S, Gregorio CC. Muscle-specific RING finger-2 (MURF-2) is important for microtubule, intermediate filament and sarcomeric M-line maintenance in striated muscle development. *Journal of cell science* 2004;117:3175–3188. [PubMed: 15199100]
56. Gomes ER, Jani S, Gundersen GG. Nuclear movement regulated by Cdc42, MRCK, myosin, and actin flow establishes MTOC polarization in migrating cells. *Cell* 2005;121:451–463. [PubMed: 15882626]
57. Von Dassow G, Odell GM. Design and constraints of the *Drosophila* segment polarity module: robust spatial patterning emerges from intertwined cell state switches. *The Journal of experimental zoology* 2002;294:179–215. [PubMed: 12362429]
58. Alberts, B.; Johnson, A.; Lewis, J.; Raff, M.; Roberts, K.; Walter, P. *Molecular Biology of the Cell*. Vol. 4. Garland Science; New York: 2002.
59. Reda T, Blumenthal R, Muller P, Herrmann A. Influence of the spectrin network on fusion of influenza virus with red blood cells. *Molecular membrane biology* 1995;12:271–276. [PubMed: 8520628]
60. Eggert US, Mitchison TJ, Field CM. Animal cytokinesis: from parts list to mechanisms. *Annual review of biochemistry* 2006;75:543–566.
61. Vitale ML, Seward EP, Trifaro JM. Chromaffin cell cortical actin network dynamics control the size of the release-ready vesicle pool and the initial rate of exocytosis. *Neuron* 1995;14:353–363. [PubMed: 7857644]
62. Chen A, Leikina E, Melikov K, Podbilewicz B, Kozlov M, LV C. Fusion pore expansion during syncytium formation is restricted by an actin network. *Journal of cell science*. 2008in press

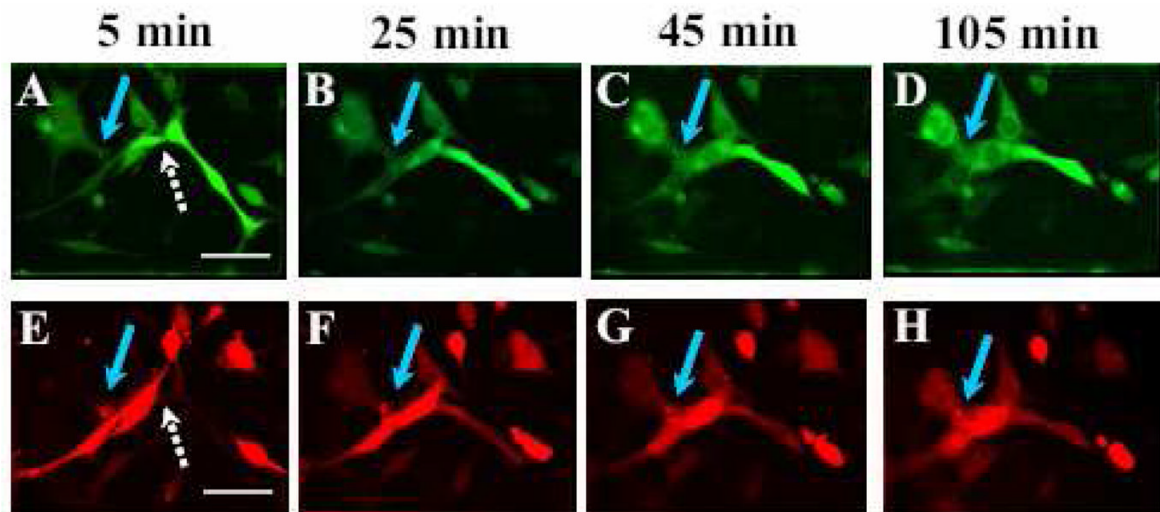


Figure 1.

Low pH application results in a fast opening of a fusion pore followed by a much slower syncytium development. Co-plated cells pre-labeled with either orange or green cell tracker were treated with a 5-min low pH pulse. Then, starting immediately after re-neutralization, we took pictures to follow redistribution of the probes between differently labeled cells (a hallmark of fusion pore formation), and gradual enlargement of intercellular connections and changes in cell shapes. The white arrows in A and E indicate a cell pair where the 2 dyes are already mixing, but each of the cells remains an individualized entity. The blue arrows mark the intercellular connection that expands from A to D and from A' to D' when adjacent fusing cells join in a big syncytium. The pictures were taken at $t=5$ min (A, A'); 25 min (B, B'); 45 min (C, C'); 105 min (D, D') after the beginning of low pH application. Scale bar, $50\mu\text{m}$.

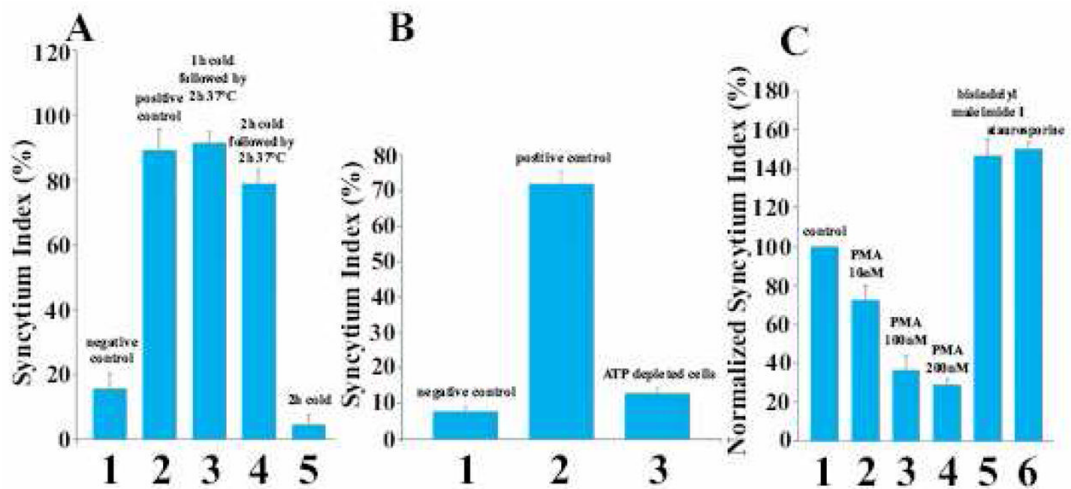


Figure 2.

Syncytium formation proceeds only in metabolically active cells and is negatively regulated by PKC.

A, B. To test whether cell-cell fusion is an energy dependent process, we placed the cells at 4°C immediately after the end of low pH pulse (A) or pre-treated them with an ATP-depleting mix of sodium azide (5 mM) and 2-D-deoxyglucose (5 mM) in PBS [59] (B). A. In the control experiments cells were kept at 37°C throughout experiment and either treated (2) or not treated (1) with low pH. (3) Low pH pulse applied at 37°C was followed by a 2 hour incubation at 4°C and then scoring syncytia. For the cold-recovery experiments, cells were kept at 4°C for 1 (4) or 2 h (5), and then were incubated for two more hours at 37°C before monitoring of the syncytium index.

B. In the control experiments, the cells that were not ATP-depleted were either treated (2) or not treated (1) with low pH. (3) cells were preincubated in the ATP-depleting mix for 30 min prior to low pH application and kept under ATP-depleting conditions throughout the experiment.

C. To explore whether low pH-triggered syncytium formation involves protein kinases activities, immediately after re-neutralization we applied PKC-modifying reagents PMA (2–4); bisindolylmaleimide I at a final concentration of 500 nM (5), and staurosporine at a final concentration of 20 nM (6). (1) Control with no reagents applied.

All bars are mean + S.E..

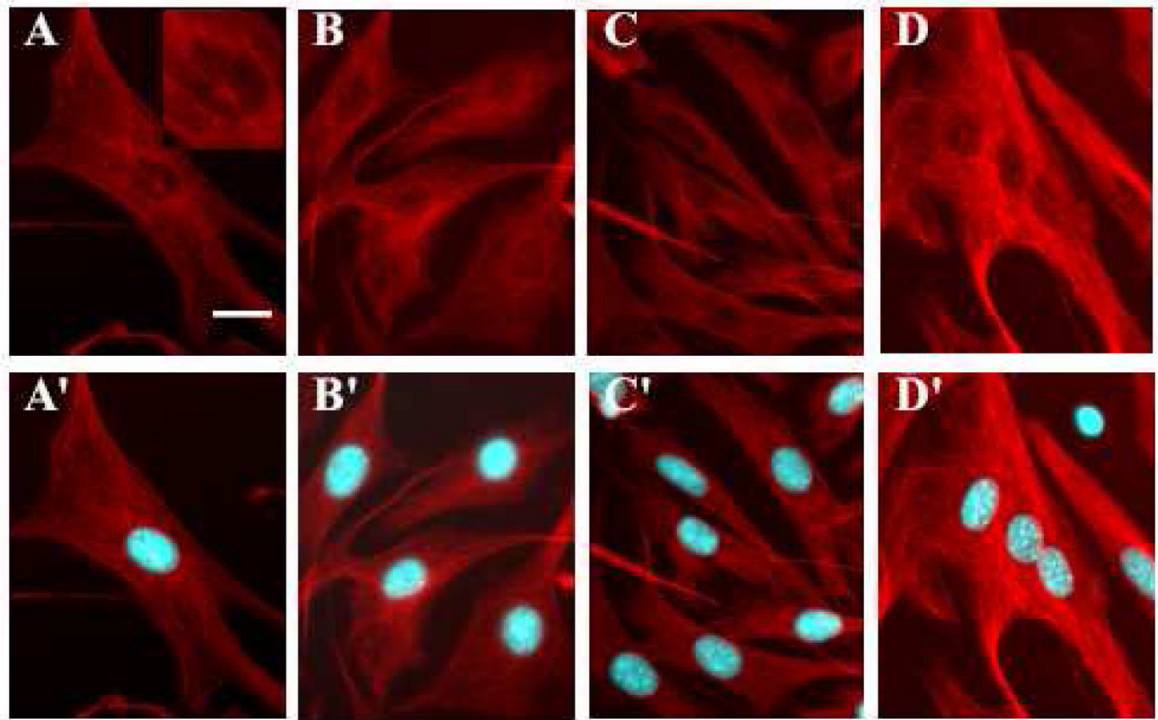


Figure 3.

Syncytium formation is accompanied by restructuring of microtubule network and loss and relocation of MTOC.

To explore the changes in the structure of microtubule skeleton during cell-cell fusion, the fusing cells were fixed at different times after low pH application. Microtubules were labeled in red with mouse anti-alpha tubulin antibody (with alexa594 donkey anti-mouse antibody as secondary antibody) and nuclei were labeled in blue with Hoechst. (A, A') the negative control without low pH application. (B–D and B'–D') Images were taken at t=5 min (B, B'); 10 min (C, C'); and 125 min (D, D') after the beginning of low pH application. For each pair of images, the second image (images A', B', C', D') includes the superimposition of the nuclei, which helps in distinguishing single and multinucleated cells, and clarifying the position of the nuclei in the syncytia, but can hide the MTOC. Scale bar, 25 μ m.

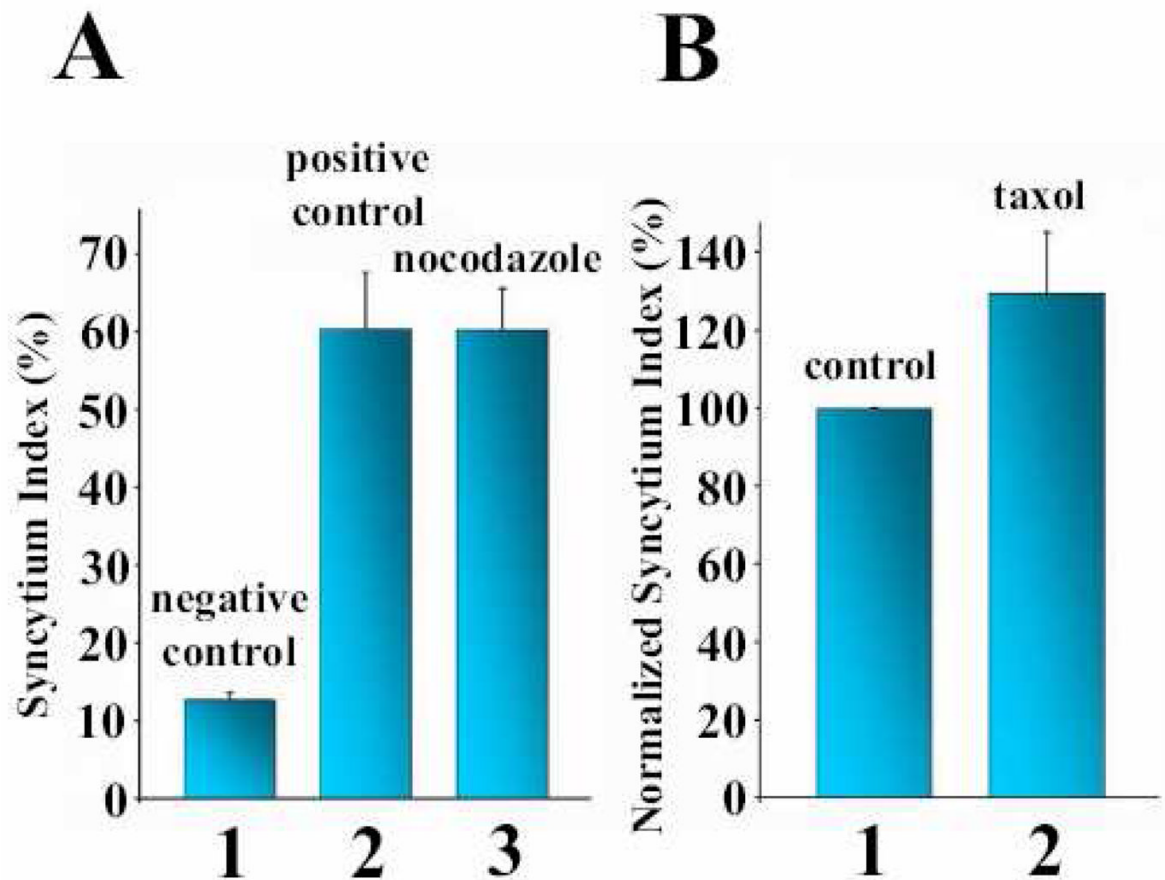


Figure 4.

Syncytium formation is unaffected by microtubule-modifying reagents. Nocodazole (A) and taxol (B) were used at final concentrations of 20 μM and 50 μM , respectively, with a preincubation time of 1 h followed by a low pH application. After 2 more hours in the presence of the reagent, syncytium formation was scored. In the control experiments, untreated cells were either exposed (A2, B1) or not exposed (A1) to low pH medium. All bars are mean + S.E..

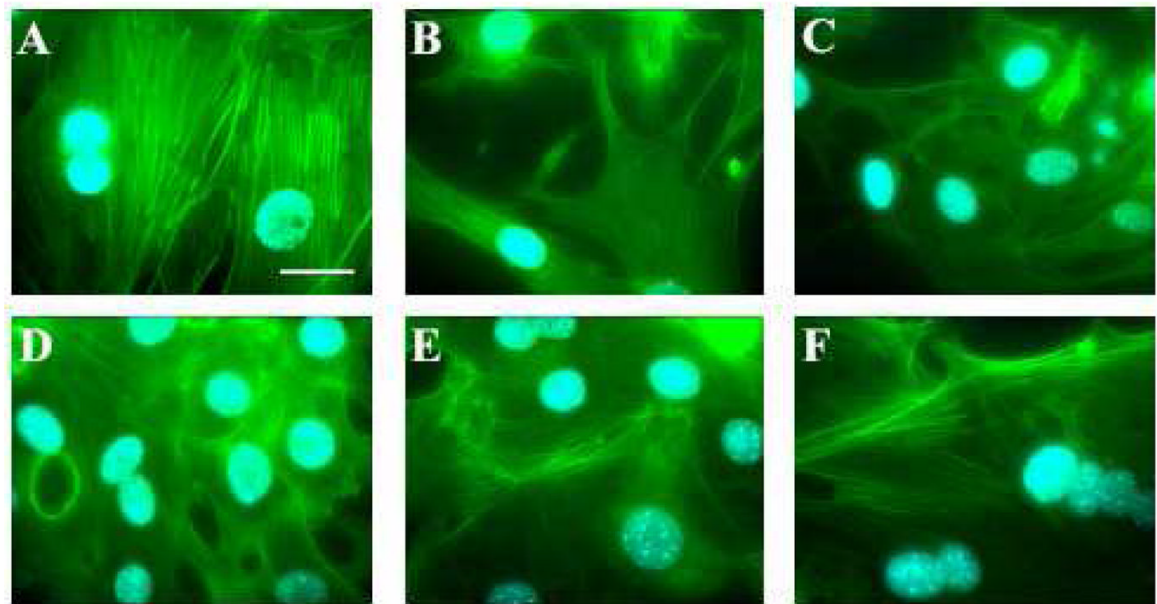


Figure 5. Reorganization of initially disassembled actin cytoskeleton during syncytium formation. Time-lapse experiments follow changes in actin cytoskeleton after its initial dissociation caused by trypsin pretreatment, through low pH-induced cell-cell fusion. At different times after low pH application the cells were fixed and labeled with Alexa488-Phalloidin and nuclei were labeled in blue with Hoechst. A is the control with non treated cells. B shows cells at the end of low pH application. Figure 5C, D, E and F: 5, 15, 60, 120 minutes after the end of low pH application. Scale bar, 20 μ m.

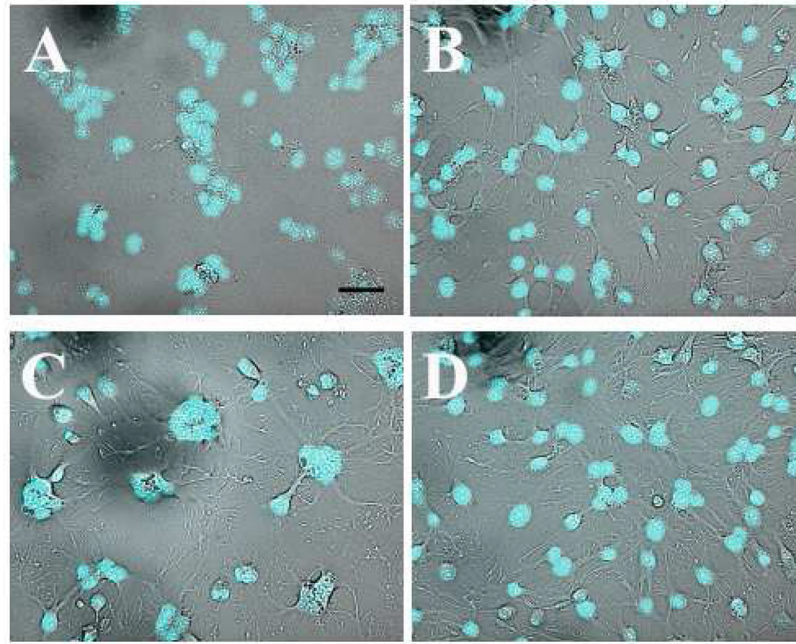


Figure 6. Disturbance of actin structures with jasplakinolide, latrunculin, and cytochalasin D does not block syncytium formation. Latrunculin A (panel B), jasplakinolide (panel C), and cytochalasin D (panel D) were used respectively at final concentrations of 2 μ M, 3 μ M, and 5 μ M with a preincubation time of 30 min. After low pH application, the cells were kept in the presence of the reagents until scoring syncytia. Panel A shows the positive control, where the syncytium totally covered the field observed. B–D. Syncytia are still formed in the presence of actin-modifying agents. Scale bar, 50 μ m.

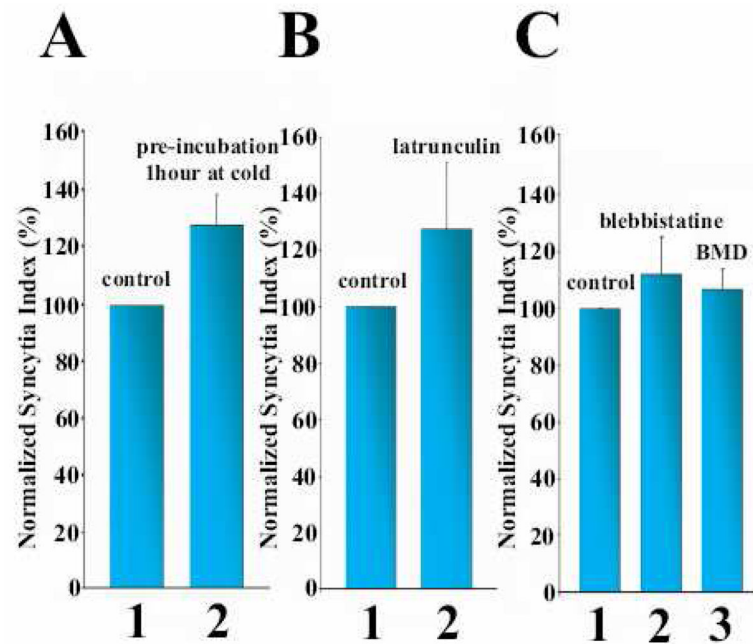


Figure 7.

Depolymerization of actin (A, B) and myosin inhibitors (C) did not lower the efficiency of syncytium formation. A. To depolymerize actin structures, the cells were preincubated for 1 h at 4°C before low pH application at 37°C (2). In the control experiment (1) the low temperature pre-treatment was skipped. B. A possible recovery of actin structures after raising the temperature was prevented by following low temperature treatment with latrunculin A application. After low pH application at 37°C, the cells were kept for 1 h at 4°C in complete medium, then the medium was replaced with a warm medium containing 2 μM latrunculin A (2) or, in the control experiment (1), latrunculin – free medium. The cells were incubated for two more hours at 37°C before quantifying the syncytium formation. C. Incubation of the cells with inhibitors of non-muscle myosin II: blebbistatin at 100 μM (2) or butanedione monoxime, BMD at 10 mM (3), started 30 and 15 min, prior to trypsin application and then kept throughout the experiments, respectively, had no effect on syncytium formation, as compared with that in the control experiment without inhibitors (1).

All bars are mean + S.E..